Computer Physics Communications 129 (2000) 13–20

Computer Physics Communications

www.elsevier.nl/locate/cpc

Dynamic structure factor in single- and two-species thermal GBL lattice gas

D. Dubbeldam [1], A.G. Hoekstra [2], P.M.A. Sloot *

University of Amsterdam, Faculty for Mathematics, Computer Science, Physics, and Astronomy, Kruislaan 403, 1098 SJ Amsterdam, The Netherlands

Abstract

The two-dimensional 19-bits GBL lattice gas model conserves energy in a non-trivial way, allowing temperature, temperature gradients, and heat conduction. We describe the thermodynamics of the model, its equilibrium properties, and confirm the change of sound speed with energy density at fixed density with simulation results. The sound speed, the sound damping, and the thermal diffusivity are extracted from the dynamic structure factor and shown for various energy densities at fixed density. We have extended the 19 bits GBL model with multiple-species (miscible fluid model) and have measured the dynamic structure factor for this two-component thermal lattice gas model.

PACS: 47.11.+j; 07.05.+t

Keywords: Lattice-gas method; GBL-model; Dynamic structure factor; Multiple-species

1. Introduction

Lattice-gas automata (LGA) are a relative novel method to simulate the hydrodynamics of incompressible fluids [1,2]. The flow is modeled by particles which reside on nodes of a regular lattice. The extremely simplified dynamics consists of a streaming step where all particles move to a neighboring lattice site in the direction of their velocities, followed by a collision step, where different particles arriving at the same node interact and possibly change their velocity according to collision rules. The main features of the model are exact conservation laws, unconditional stability, a large number of degrees of freedom, intrinsic spontaneous fluctuations, low memory consumption, and the inherent spatial locality of the update rules, making it ideal for parallel processing [3].

The LGA seem most suitable for the study of non-equilibrium fluctuations. The study of fluctuations in a fluid subjected to a temperature gradient is very interesting. This would require the implementation of energy boundaries. Here we restrict ourself to the simple case of a fluid at global equilibrium and investigate the transport properties at different energy densities.

* Corresponding author. E-mail: sloot@wins.uva.nl.

[1] E-mail: dubbelda@wins.uva.nl.

[2] E-mail: alfons@wins.uva.nl.

0010-4655/00/$ – see front matter
PII: S0010-4655(00)00088-6

The introduction of thermal properties requires multiple velocities. The 19-bits model proposed by Grosfils, Boon, and Lallemand (GBL model) has 19 velocities and is the subject of this paper. We will describe the thermodynamics of this specific lattice gas system and investigate some of its properties, like the speed of sound, sound damping, and thermal diffusivity, all as a function of energy density.

We start by defining the lattice gas b-bit (thermal) models. We numerically calculate the speed of sound from the theoretical equations and verify this with the speed of sound as obtained from measurements of the dynamical structure factor from simulation. The calculated numerical solution of the Fermi–Dirac equations enables us to specify energy independent of density.

Finally, we have extended the GBL model with multiple species (miscible fluids) and show that the spectra of such systems are enhanced with a extra contribution arising from diffusion.

2. Lattice-gas model

The two-dimensional b-bits lattice-gas model is based on a triangular lattice, containing $V = L^d$ (d is the dimensionality of the model, L the lattice size) nodes (also interpreted as the volume of the lattice). The state of a single node $\mathbf{r} \in V$ is given in terms of Boolean occupation numbers $\mathbf{n}_i(\mathbf{r}, t) \in \{0, 1\}$ denoting the absence/presence of a particle in velocity channel $(\mathbf{r}, \mathbf{c}_i)$, $i = 1, 2, \ldots, b$ at time t. The particles have unit mass with no spatial extension, and behave as a simplified version of a classical hard-sphere gas. The model is an iterative two-step sequence of propagation and collision, formalized in the following dynamical rule:

$$n_i(\mathbf{r} + \mathbf{c}_i, t + 1) = n_i(\mathbf{r}, t) + \Delta\ \mathbf{n}_i(\mathbf{r}, t)\big), \quad i = 1, \ldots, b, \tag{1}$$

where $\Delta(\mathbf{n}(\mathbf{r}, t))$ is the collision operator, conserving mass, momentum, and energy. The exclusion principle (no more than one particle is allowed at a given time in a certain channel) leads to Fermi–Dirac statistics of the system.

The average occupation number $f(\mathbf{r}, \mathbf{c}_i, t)$ of a particle state with velocity $\mathbf{c}$ at site $\mathbf{r}$ satisfies the nonlinear Boltzmann equation

$$f(\mathbf{r} + \mathbf{c}_i, \mathbf{c}_i, t + 1) = f(\mathbf{r}, \mathbf{c}_i, t) + \Delta\ f(\mathbf{r}, \mathbf{c}_i, t)\big). \tag{2}$$

The local density ρ, the velocity $\mathbf{u}$, the energy density e, and the corresponding internal energy density e_{int} are defined as

$$\rho(\mathbf{r}, t) = \sum_{i=1}^{b} f(\mathbf{r}, \mathbf{c}_i, t), \qquad \mathbf{u}(\mathbf{r}, t) = \frac{\sum_{i=1}^{b} \mathbf{c}_i f(\mathbf{r}, \mathbf{c}_i, t)}{\rho(\mathbf{r}, t)},$$

$$e(\mathbf{r}, t) = \frac{\sum_{i=1}^{b} \frac{1}{2}\mathbf{c}_i^2 f(\mathbf{r}, \mathbf{c}_i, t)}{\rho(\mathbf{r}, t)},$$

$$e_{\text{int}}(\mathbf{r}, t) = \frac{\sum_{i=1}^{b} \frac{(\mathbf{c}_i\ \mathbf{u})^2}{2} f(\mathbf{r}, \mathbf{c}_i, t)}{\rho(\mathbf{r}, t)} = e(\mathbf{r}, t) \quad \tfrac{1}{2}\ \mathbf{u}(\mathbf{r}, t)\big)^2. \tag{3}$$

3. Thermodynamics

The stationary equilibrium distribution obeys Fermi–Dirac statistics. The average occupation of a single particle state with velocity $\mathbf{c}$ at site r is given by:

$$f(\mathbf{r}, \mathbf{c}_i, t) = \big\langle n(\mathbf{c}_i, t)\big\rangle = \frac{1}{1 + \mathrm{e}^{\ \alpha + \frac{1}{2}\beta c_i^2\ \ \gamma \mathbf{c}_i}}, \tag{4}$$

where $\frac{\alpha}{\beta}$ is the chemical potential, $\beta = \frac{1}{k_B T}$ is the inverse temperature, γ is the conjugate to the velocity flow, $\mathbf{c}_i$ the velocity vector, and c_i the velocity channel i. If we restrict ourself to stationary equilibrium the γ parameter vanishes ($\mathbf{u} = \gamma = 0$). The reduced temperature θ and fugacity z are defined as

$$\theta = e^{\frac{1}{2}\beta}, \qquad z = e^{\alpha} \quad (\theta > 0, z > 0). \tag{5}$$

The density and energy equations (3) can be used to numerically calculate z and θ from ρ and ρe. Once we have z and θ, we know α and β, and hence also $f(\mathbf{r}, \mathbf{c}_i, t)$ for all i's. The equilibrium properties of the thermal lattice gases, such as pressure p, entropy per particle s, and the sound velocity c_s are [4,5]:

$$p(\mathbf{r}, t) = \frac{1}{d}\sum_{i=1}^{b}(\mathbf{c}_i \quad \mathbf{u})^2 f(\mathbf{r}, \mathbf{c}_i, t) = \frac{2}{d}\rho(\mathbf{r}, t) e_{\text{int}}(\mathbf{r}, t), \tag{6}$$

$$s(\mathbf{r}, t) = \frac{\sum_{i=1}^{b}(f(\mathbf{r}, \mathbf{c}_i, t)\ln(f(\mathbf{r}, \mathbf{c}_i, t)) + (1 \quad f(\mathbf{r}, \mathbf{c}_i, t))\ln(1 \quad f(\mathbf{r}, \mathbf{c}_i, t)))}{\rho(\mathbf{r}, t)}, \tag{7}$$

$$c_s = \sqrt{\frac{1}{d}\frac{\sum_{i=1}^{b} c_i^4 \kappa(c_i)}{\sum_{i=1}^{b} c_i^2 \kappa(c_i)}}, \quad \kappa(c_i) = f(\mathbf{r}, \mathbf{c}_i, t)\ 1 \quad f(\mathbf{r}, \mathbf{c}_i, t)\big), \tag{8}$$

where κ is the fluctuation in the occupation number.

4. The 19-bits GBL model

The thermal 19-bits model proposed by Grosfils et al. defines multi speed dynamics on a triangular lattice [6]. It has four velocity magnitudes: 1 rest particle with velocity 0, 6 particles with velocity 1, 6 particles with velocity $\sqrt{3}$, and 6 particles with velocity 2 (see Fig. 1(a)). The corresponding energy values of the particles are 0, $\frac{1}{2}$, $\frac{3}{2}$ or 2 and are purely kinetic. In the collision step the output state is randomly chosen among all states having the same mass, momentum, and energy, as the input state.

The average density ρ and the energy density e for the 19-bits GBL model in stationary equilibrium can be written as [7] (similar as for 9-bits square lattice gas [4]):

$$\rho(\mathbf{r}, t) = \sum_{i=1}^{19} f(\mathbf{r}, \mathbf{c}_i, t) = \frac{z}{1+z} + \frac{6z\theta}{1+z\theta} + \frac{6z\theta^3}{1+z\theta^3} + \frac{6z\theta^4}{1+z\theta^4}, \tag{9}$$

$$\rho(\mathbf{r}, t) e(\mathbf{r}, t) = \sum_{i=1}^{19} \frac{1}{2}\mathbf{c}_i^2 f(\mathbf{r}, \mathbf{c}_i, t) = \frac{3z\theta}{1+z\theta} + \frac{9z\theta^3}{1+z\theta^3} + \frac{12z\theta^4}{1+z\theta^4}. \tag{10}$$

An example of the solution of these equations is shown in Fig. 1(b). Here we plot the occupation numbers for a fixed reduced density of 0.25 over the total energy density range. Note that at higher densities not all energy density are possible. This is a consequence of the finite number of velocity channels in the system. Fig. 1(d) shows the total range of reduced density versus energy density which is realizable in the 19 bits model.

The precise definition of temperature in a lattice-gas system is far from trivial. The assumption of a local version of the equi-partition theorem leads to the tempting definition of $e = \frac{d}{2}T$. However as Cercignani [8] and Ernst [5] point out, this step is purely formal and not related at all to the physical meaning of temperature. The definition of $T = \frac{1}{\beta}$ however leads to the notion of negative absolute temperatures (the energy is bounded from above). Fig. 1(c) shows the temperature T and the inverse temperature β a function of the internal energy as obtained from the solution of Eqs. (9) and (10). Here we clearly see the strong non-linear relation between e_{int} and T. Note also that at energy density $e = \frac{24}{19}$ (where all occupation numbers have equal value) the temperature is ill-defined. Temperature is *not* an easy concept in lattice-gas systems, and a more natural parameter is the energy density.

The $e = \frac{24}{19}$ is a special point where all occupation numbers have the same value. This point is independent of the density of the LGA. It is the only energy density, where the sound speed is fixed (at $\frac{1}{4}\sqrt{26}$), and does not vary with density.

5. Transport coefficients

The Boolean microscopic nature, combined with stochastic micro-dynamics, results in intrinsic spontaneous fluctuations in LGA [6,9,10]. These fluctuations can be described by the dynamic structure factor $S(\mathbf{k},\omega)$, the space and time Fourier transform of the density autocorrelation function [11], and occur with a distribution of wavelengths $\mathbf{k}$ and frequencies ω.

$S(\mathbf{k},\omega)$ of real fluids can be measured by light-scattering experiments, where the measured quantity is the power spectrum of density fluctuations. The dynamic structure factor $S(\mathbf{k},\omega)$ for real fluids in the Landau–Placzek approximation (small values of k and ω) reads [11]:

$$\frac{S(\mathbf{k},\omega)}{S(\mathbf{k})} = \left(\frac{\gamma \quad 1}{\gamma}\right)\frac{2\chi k^2}{\omega^2 + (\chi k^2)^2} + \frac{1}{\gamma}\sum_{\pm}\frac{k^{\,2}}{(\omega \pm c_s k)^2 + (\ k^{\,2})^2}$$
$$+\frac{1}{\gamma}[\quad +(\gamma \quad 1)\chi]\frac{k}{c_s}\sum_{\pm}\frac{c_s k \pm \omega}{(\omega \pm c_s k)^2 + (\ k^{\,2})^2}, \tag{11}$$

where $S(\mathbf{k})$ is the static structure factor. Here χ is the thermal diffusivity, $\quad = \frac{1}{2}[\nu + (\gamma \quad 1)\chi]$ the sound damping, where ν is the longitudinal viscosity, c_s is the adiabatic sound speed, and γ is the ratio of specific heats. A typical spectrum as found in real fluids consists of three spectral lines, a central peak (Rayleigh peak), which arises from entropy fluctuations at constant pressure and corresponds to the thermal diffusivity mode, and two shifted peaks (Brillouin peaks), which arise from pressure fluctuations at constant entropy and correspond to the acoustic modes.

Eq. (11) for $S(k,\omega)$ is known as the Landau–Placzek approximation and also holds for the GBL model in the limit for small k and small ω [6,9]. A measured spectrum from a GBL simulation contains transport coefficient information. We can extract the sound damping as the half-width of the Brillouin peaks: $\Delta\omega = \ k^{\,2}$. We measure, by simulation, $\Delta\omega$ as a function of k^2. A least-square fit provides the value of the slope, which is an experimental value of .

The thermal diffusivity coefficient χ is obtained as the half-width of the central peak: $\Delta\omega = \chi k^2$. The experimental determination of the position of the Brillouin peaks is a measurement of the adiabatic sound velocity c_s. The ratio of the specific heats γ can be obtained as the ratio of the integrated intensity of the Rayleigh peak to those of the Brillouin peaks. The transport coefficients for a fixed reduced density 0.25 for various energy densities are shown in Fig. 2. They are extracted from the spectra as obtained from simulations at fixed reduced density of 0.25, 1,000,000 timesteps, at a gridsize of 512 × 512. The results are a fit over all points in the hydrodynamical regime. For details of the simulations we refer to [3].

Fig. 3 shows three spectra at $k_x = 0.098$ and fixed reduced density 0.25, but for different energy densities 0.6, 0.8, and 1.0. We clearly see the different $\omega_{\max}$, corresponding to $c_s k$, and the different ratio of the ares of the central peaks and Brillouin peaks. The width at half height differences are less clear to see. The spectra become noisier as $\mathbf{k}$ increases (Fig. 3(b)), hence accuracy of the measurements decreases for larger $\mathbf{k}$. However at low $\mathbf{k}$, the accuracy decreases with $\mathbf{k}$, since it depends on the frequency resolution $\Delta\omega = 2\pi/T$ (T the number of time iterations). In practice this means the first few $\mathbf{k}$ should be skipped. Better accuracy can be achieve by a longer simulation time. The time Fourier transform is taken over intervals of 16,384 time steps, and the intervals are half-overlapped (subsequential intervals are not totally uncorrelated, but half-overlapping seems to be a good choice [12]). For our simulation time of 1,000,000 timesteps this means we have 122 intervals, and the initial variance is reduced by $\sqrt{122}$. The spectrum at $k = 0.49$ of Fig. 3(b) is inside the hydrodynamical regime and is raw data (no smoothing).

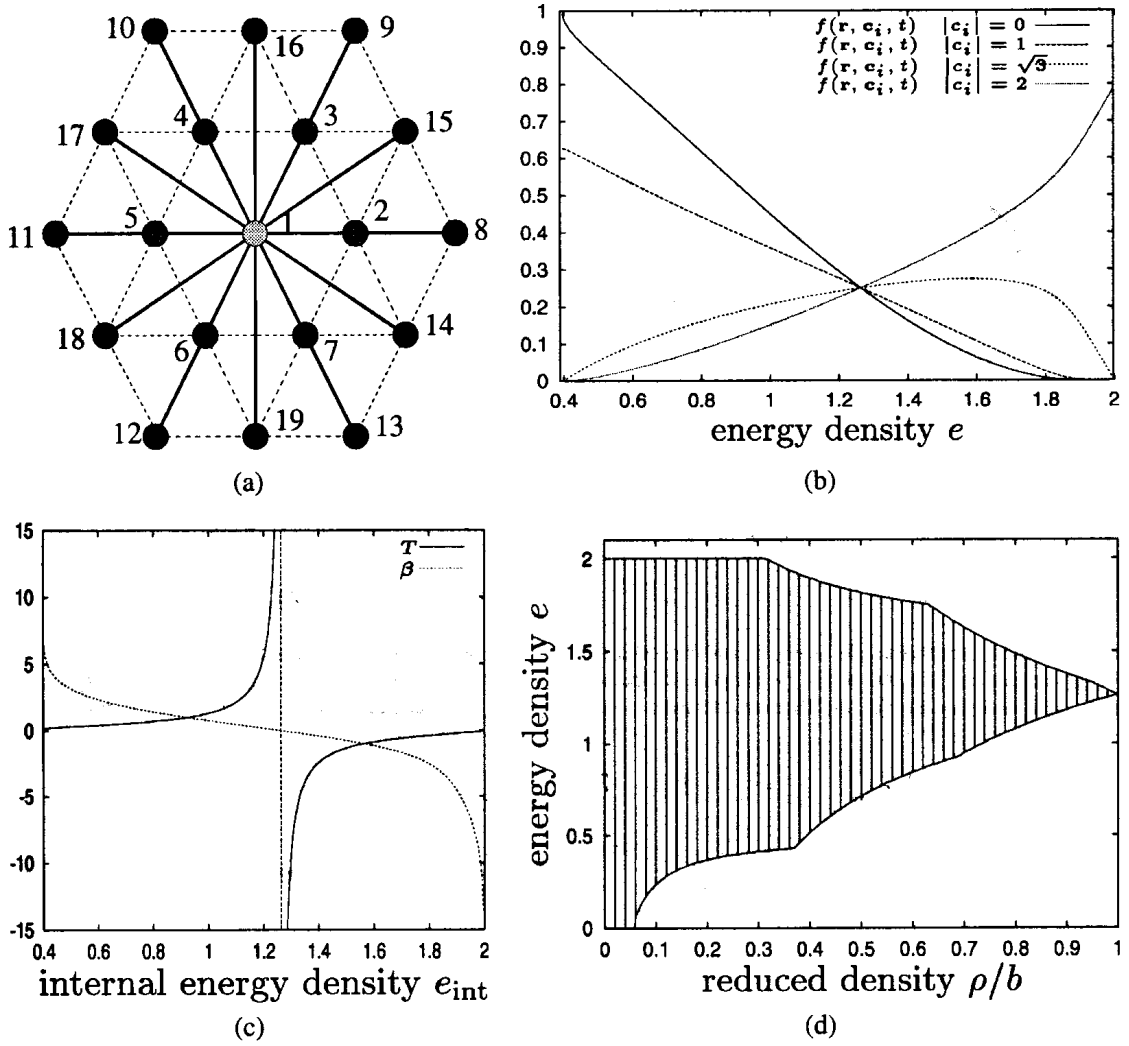

Fig. 1. The 19 bits GBL model has a spatial arrangement of the 19 velocity as shown in (a). There are four velocity magnitudes 0, 1, $\sqrt{3}$, and 2. Figure (b) shows the occupation number for these four groups as a function of energy density for a reduced density of 0.25 at global equilibrium. Figure (c) shows that the definition $T = \frac{1}{\beta}$ leads to a negative absolute temperature for $e > \frac{24}{19}$. Figure (d) shows which combinations of density and energy are realizable in the GBL model. (a) Spatial arrangement of the 19 occupation numbers $f(\mathbf{r}, \mathbf{c}_i, t)_{i=1..19}$. (b) Occupation numbers for the four different velocity magnitudes. The special point where all f_i's are equal is located at $e = 24/19$. (c) Temperature T and inverse temperature β as a function of internal energy e_{int}. (d) Simulation-range density vs. energy.

6. The spectrum of a two component thermal lattice gas

A miscible two-component lattice gas is easily constructed. The particles are tagged with a different color, red and blue. The collision step is followed by a random redistribution of the colors. We use a parallel implementation of the multi-species thermal GBL model (including the FFT-analysis), which is efficient and has good scalability [3].

The $S(k, \omega)$ for a two-component system has a spectrum structure where it is difficult to separate the contributions from concentration fluctuations and entropy fluctuations [11]. The two contributions are independent if one of the two components is in trace amounts, but in general the two are not decoupled.

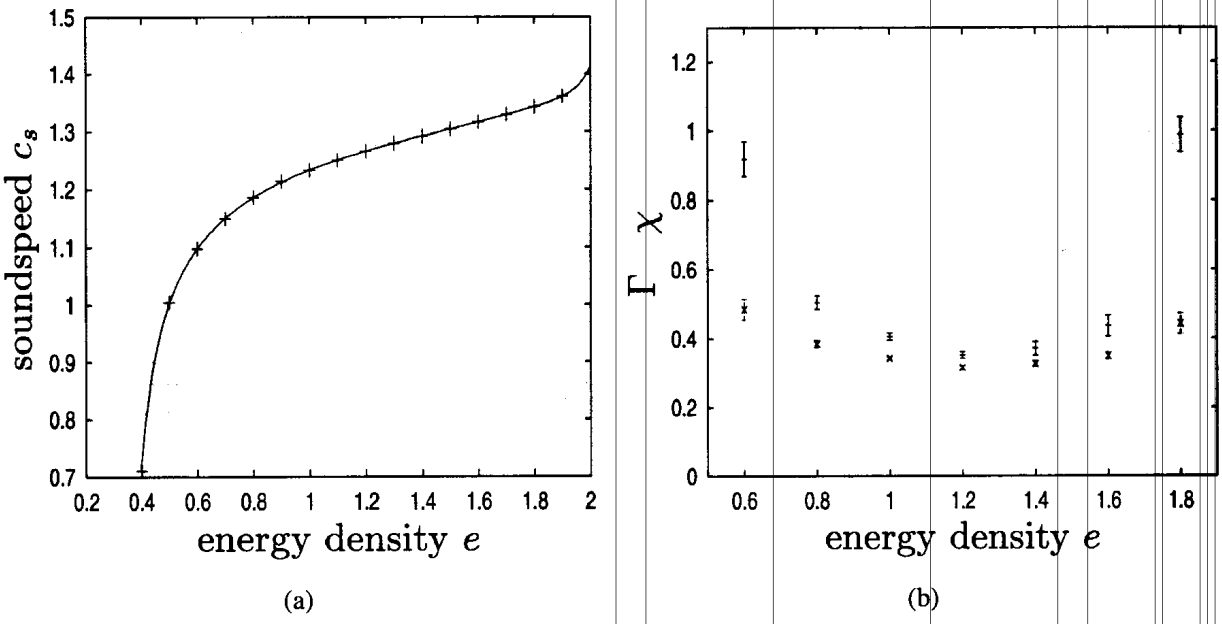

(a) (b)

Fig. 2. The speed of sound c_s, the thermal diffusivity χ, and the sound damping as obtained from simulation. The reduced density is fixed at 0.25, the number of iterations is 1,000,000 on a 512×512 grid. (a) Speed of sound c_s (errorbars too small to be seen). The crosses are simulation results, the solid line from theory, Eq. (8). (b) Thermal diffusivity χ (upper points) and sound damping (lower points), as measured from simulation.

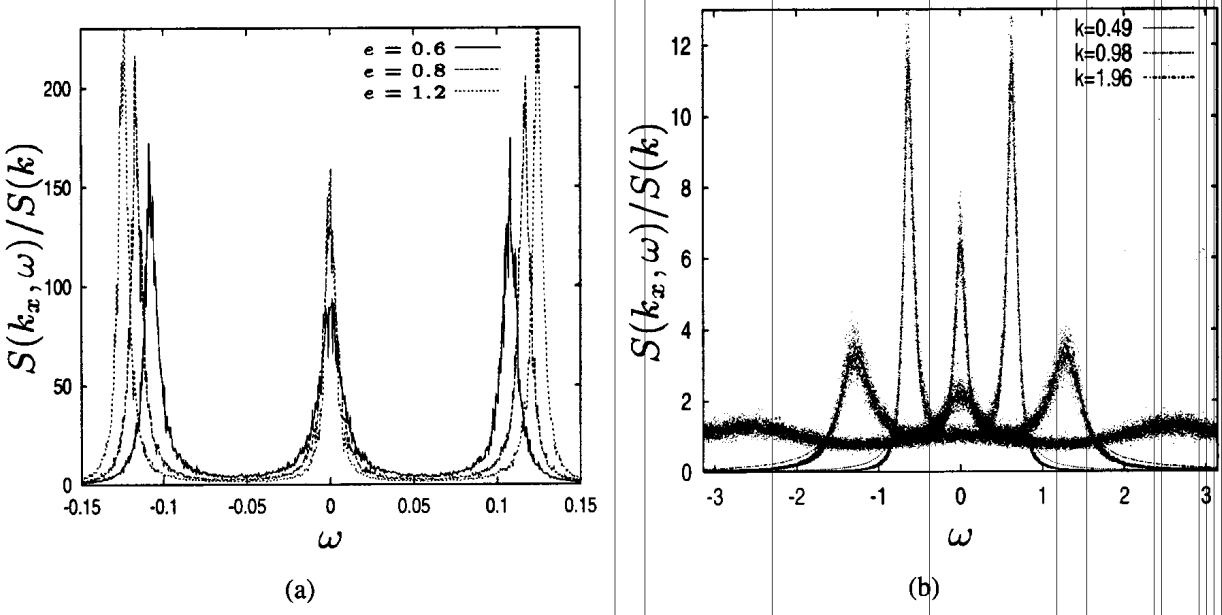

(a) (b)

Fig. 3. Spectra at different energy densities (fixed density) and different k's. Spectra scaled as $\int_{\pi}^{\pi} S(\mathbf{k},\omega)\,d\omega = 2\pi S(\mathbf{k})$. (a) Spectra at $k_x = 0.098$ for three energy densities 0.6, 0.8 and 1.2 at fixed reduced density 0.25 (raw data, not smoothed). (b) Spectra at $k_x = 0.49$, 0.98, 1.96 (highest is 0.49, lowest is 1.96).

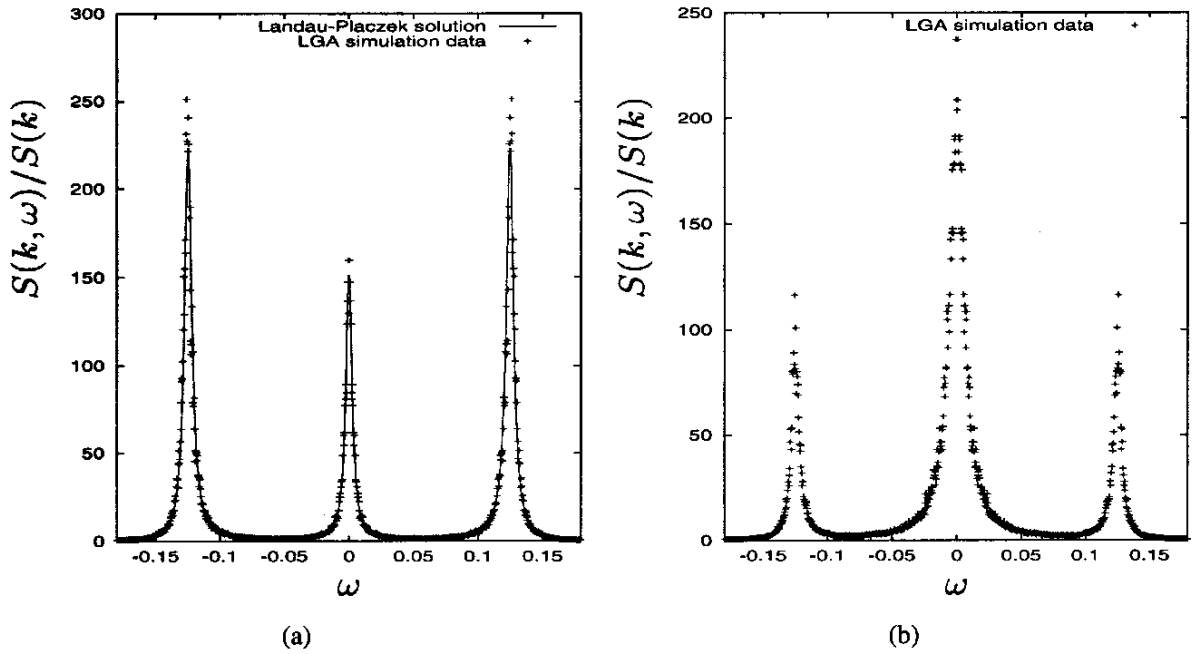

Fig. 4. The spectral function $S(k,\omega)$ for (a) 100% and (b) 50% red GBL lattice gas ($k_x = 8 \times \frac{2\pi}{512}$, reduced density 0.25, energy density 1.3), data obtained from 1,000,000 timesteps. (a) 100% red particles. (b) 50% red particles.

Fig. 4(a) shows $S(k,\omega)$ for the standard GBL model. The simulation data obtained from the lattice gas simulation is fitted with the analytical solution, providing the transport coefficients in lattice units. Fig. 4(b) shows $S(k,\omega)$ for the two-species GBL model. We notice a significant contribution from concentrations fluctuations to the amplitude of the Rayleigh peak.

7. Conclusion

The 19-bits GBL model possesses thermal properties, which can be investigated more closely now that we can specify the energy density independent from densities by numerically solving the equations resulting from the Fermi–Dirac statistics. We have verified the change of sound speed with energy density (fixed density) from simulation with the theoretical values, and find good agreement. We are now able to specify no-slip thermal boundaries, which we will be using to investigate heat-conduction, Rayleigh–Bernoulli convection, Poiseuille flow with walls at different temperatures etc. In our opinion the 19 bits model is still useful and interesting for the simulation of non-equilibrium phenomena.

Another research topic is the extension of the GBL-model into a multiple species model. We have shown a spectrum as a preliminary result.

References

[1] U. Frish, B. Hasslacher, Y. Pomeau, Lattice-gas automata for the Navier–Stokes equation, Phys. Rev. Lett. 56 (1986) 1505.
[2] D.H. Rothman, S. Zaleski, Lattice Gas Cellular Automata (Cambridge University Press, 1997).
[3] D. Dubbeldam, A.G. Hoekstra, P.M.A. Sloot, Computational aspects of multi-species lattice-gas automata, in: Lecture Notes in Computer Science, Vol. 1593 (Springer, Berlin, 1999), pp. 339–349.

[4] S. Das, M.H. Ernst, Thermal transport properties in a square lattice gas, Physica A 187 (1992) 191–209.
[5] M.H. Ernst, S. Das, Thermal cellular automata fluids, J. Statist. Phys. 66 (1991) 465–483.
[6] P. Grosfils, J.P. Boon, P. Lallemand, Spontaneous fluctuation correlations in thermal lattice-gas automata, Phys. Rev. Lett. 68 (1992) 1077–1080.
[7] P. Grosfils, Hydrodynamique statistique des gaz sur resau, Ph.D. thesis, Universite Libre de Bruxelles (June 1994).
[8] C. Cercignani, Temperature, entropy, and kinetic theory, J. Statist. Phys. 87 (1996) 1097–1109.
[9] P. Grosfils, J.P. Boon, R. Brito, M.H. Ernst, Statistical hydrodynamics of lattice-gas automata, Phys. Rev. E 48 (1993) 2655–2668.
[10] D. Hanon, J.P. Boon, Diffusion and correlations in lattice-gas automata, Phys. Rev. E 56 (1997) 6331–6339.
[11] J.P. Boon, S. Yip, Molecular Hydrodynamics (McGraw-Hill, New York, 1980).
[12] W.H. Press, B.P. Flannery, S.A. Teukolsky, W.T. Vetterling, Numerical Recipes in C (Cambridge University Press, 1988).